

## Dimensionality crossover and the nonlinear dielectric response in betaine phosphate/arsenate mixed crystals

This article has been downloaded from IOPscience. Please scroll down to see the full text article.

1996 J. Phys.: Condens. Matter 8 6095

(<http://iopscience.iop.org/0953-8984/8/33/016>)

View [the table of contents for this issue](#), or go to the [journal homepage](#) for more

Download details:

IP Address: 171.66.16.206

The article was downloaded on 13/05/2010 at 18:32

Please note that [terms and conditions apply](#).

## Dimensionality crossover and the nonlinear dielectric response in betaine phosphate/arsenate mixed crystals

Yong-Hae Kim<sup>†</sup>, Bog-Gi Kim<sup>†</sup>, Jong-Jean Kim<sup>‡§</sup>, Tomoyuki Mochida<sup>‡</sup> and Seiichi Miyajima<sup>‡</sup>

<sup>†</sup> Physics Department, Korea Advanced Institute of Science and Technology, Taejon 305-701, Korea

<sup>‡</sup> Institute for Molecular Science, Myodaiji, Okazaki 444, Japan

Received 12 April 1996

**Abstract.** Dielectric properties of quasi-one-dimensional hydrogen-bonded chains are studied for mixed crystals of antiferroelectric betaine phosphate and ferroelectric betaine arsenate at three different mixing concentrations,  $x = 0.1, 0.3,$  and  $0.4$  ( $x$  being the concentration of arsenate). For mixed crystals with  $x = 0.3$  and  $0.4$  dielectric study revealed dimensionality crossover at around 82 K, where the quasi-one-dimensional nature was turned into three-dimensional Curie–Weiss behaviour on lowering the temperature, well above the antiferroelectric transition point. For  $x = 0.1$  mixed crystal, on the other hand, the crossover point was almost coincident with the antiferroelectric transition point, showing still too-weak interchain coupling and strong one-dimensionality, almost to the point of antiferroelectric transition. For this system, the electric bias field effect revealed temperature-dependent nonlinearity of the dielectric constant, which may be ascribed to a development of competition between antiferroelectric and ferroelectric interchain couplings, the latter growing with increasing bias field and lowering temperature.

### 1. Introduction

Since the first discovery of antiferroelectricity in BP,  $(\text{CH}_3)_3\text{NCH}_2\text{COOH}_3\text{PO}_4$ , betaine phosphate, by Albers *et al* [1] betaine compounds have been of great interest to many research workers [2]. BP first attracted attention because of its antiferroelectric phase transition at 86 K without cell doubling. Subsequent x-ray [3], dielectric and Raman [4–7], elastic constant [8], and heat capacity [9] studies revealed its phase transition sequence, as follows. The highest-temperature phase with a monoclinic space group  $P2_1/m$  undergoes an antiferrodistortive transition with unit-cell doubling along the  $c$ -axis at  $T_{c1} = 365$  K to a paraelectric  $P2_1/c$  phase. After transforming into an antiferroelectric phase at  $T_{c2} = 86$  K, the crystal undergoes a third transition at  $T_{c3} = 81$  K, which is characterized by another cell doubling along the  $a$ -axis. Deuteration of acidic protons in BP does not change  $T_{c1}$ , but significantly increases  $T_{c2}$  up to 155 K [10, 11]. High-pressure work showed coalescence of  $T_{c2}$  with  $T_{c3}$  at 85.6 K when the applied pressure was reaching 8 MPa [12]. Interestingly, when a d.c. electric field was applied above a critical value,  $E_{cr} = 5.5$  kV cm<sup>-1</sup>, a field-induced ferroelectric transition took place instead of the original antiferroelectric transition [6, 13].

Betaine arsenate (BA,  $(\text{CH}_3)_3\text{NCH}_2\text{COOH}_3\text{AsO}_4$ ) exhibits a ferroelastic transition at  $T_{c1} = 411$  K and a ferroelectric transition at  $T_{c2} = 119$  K [14]. Another transition

§ On leave from KAIST, Taejon, Korea, and to whom any correspondence should be addressed.

corresponding to  $T_{c3}$  was also observed at 102 K [15]. Deuteration of acidic protons raised  $T_{c2}$  up to 172 K, but at very high deuteration, over 75%, a phase transition to an antiferroelectric phase was observed instead of the original ferroelectric transition [16, 17]. Deuteration does not affect the  $T_{c1}$ -transition, similarly to the case of BP. Schell and Müser [18, 19] analysed the temperature dependence of the dielectric function, to find that the Curie–Weiss law held only within the small temperature range  $0 < T - T_{c2} < 8$  K, but a weakly coupled one-dimensional Ising chain model was appropriate in the temperature region  $T - T_{c2} > 8$  K.

The experimental facts above reveal that in BP and BA a delicate competition exists between antiferroelectric and ferroelectric orderings, and also in the dimensionality of the interactions. The remarkable isotope effects show that the antiferroelectric and ferroelectric transitions are related to the hydrogen dynamics and ordering. These crystals have hydrogen bond chains which connect inorganic anions along the  $b$ -axis in BP [3] and the  $c$ -axis in BA [20]. No explicit interchain hydrogen bonds exist, and zwitterionic betaine molecules are connected to the anions of the chain by different hydrogen bonds directing almost perpendicular to the chain. The existence of this additional hydrogen bonding differentiates BP and BA from the prototypical hydrogen-bonded one-dimensional (1D) ferroelectric crystal, caesium dihydrogen phosphate. Although BP and BA are not isomorphous, and the two hydrogen-bonded chain axes have a considerable lattice mismatch ( $b = 7.852$  Å for BP and  $c = 8.128$  Å for BA), mixed single crystals,  $\text{BP}_{1-x}\text{A}_x$ , can be grown for almost the whole range of arsenate concentration  $x$  [21, 22]. Maeda and Suzuki performed dielectric measurements on  $\text{BP}_{1-x}\text{A}_x$  mixed crystals, and found antiferroelectric transitions for  $0 \leq x \leq 0.4$  and ferroelectric transitions for  $0.9 \leq x \leq 1.0$ , but a dipole glass phase for  $0.5 \leq x \leq 0.85$  [20].

In the present work we want to examine in more detail the dielectric responses of mixed crystals,  $\text{BP}_{1-x}\text{A}_x$ , in the region of  $x$  including the antiferroelectric/dipole glass phase boundary ( $x = 0.4$ ) and well inside the antiferroelectric phase ( $x = 0.1$  and  $0.3$ ) to understand the nature of the competing interactions and dimensionality crossover phenomenon.

## 2. Experimental procedure

The dielectric constants were measured by use of a programmable electrometer (Keithley 617) controlled by a personal computer. The quasi-static dielectric constant  $\epsilon_s$  was measured along the  $b$ -axis by applying a stepwise voltage change  $\Delta V$  across the sample capacitor  $C_s$  and measuring the accumulated charge  $\Delta Q(t)$  which has flowed out of the sample surface. The response to the stepwise voltage change is approximated by

$$\Delta Q(t) = \Delta Q_0(1 - e^{-t/\tau}) + at \quad (1)$$

where  $\tau$  was about 1 s. The second term represents a leakage current, and  $a$  was  $\sim 0.5$  pA in our system. The data on the accumulated charge typically between  $t = 3$  s and 10 s were fitted by the above equation, and  $\Delta Q_0$  was determined. We then obtained  $\epsilon_s$  from

$$\epsilon_s = \frac{\Delta P}{\Delta E} = \frac{\Delta Q_0}{A} \frac{d}{\Delta V} \quad (2)$$

where  $d$  and  $A$  denote the thickness (typically 0.7 mm) and area of the sample capacitor. In order to ensure freedom from the bias field effect and possible hysteresis we tried to remove the after-effect of  $\Delta V$  by applying a healing voltage  $V_n$  in staircase steps before applying a new  $\Delta V$ :

$$V_n = (-k)^n \Delta V \quad (3)$$

where  $n$  represents the step number increasing from  $n = 1$  to 7,  $k$  is an arbitrary fractional number (0.7 in the present work), and each step voltage was applied for as long as 5 s.

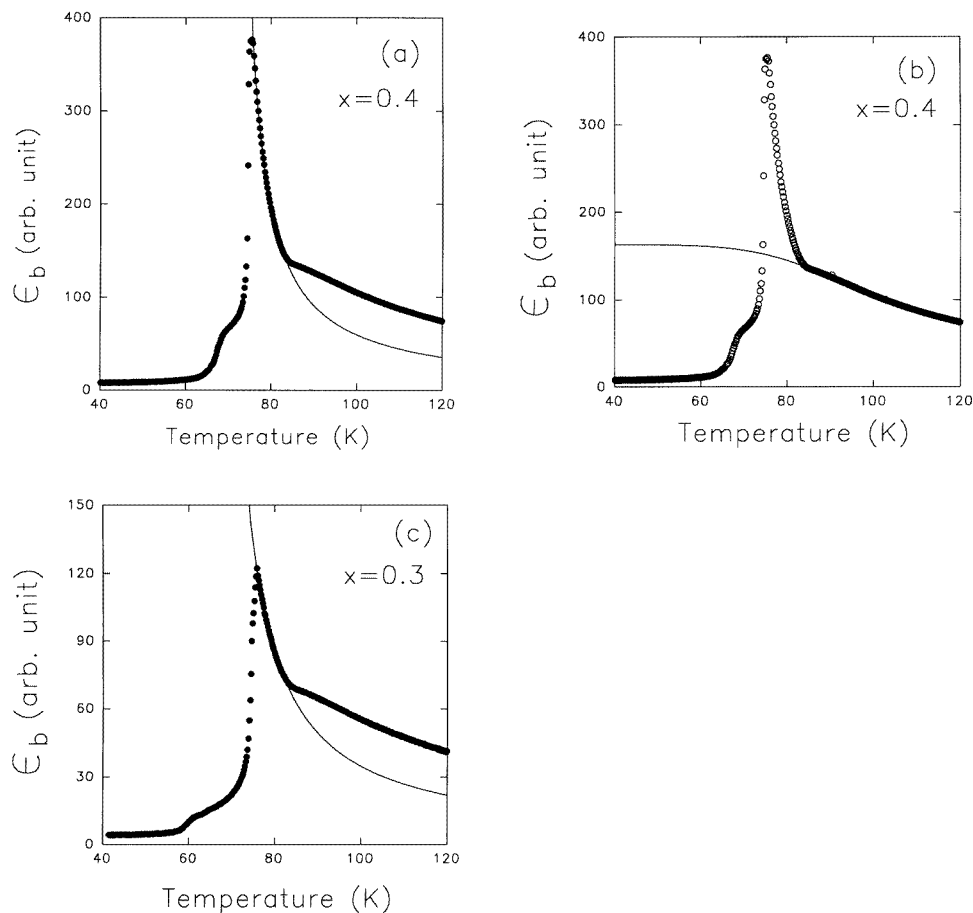


**Figure 1.** The temperature dependence of the quasi-static dielectric constant  $\epsilon_s$  for BP<sub>1-x</sub>A<sub>x</sub> mixed crystals. (a)  $x = 0.4$ ; the solid curve represents the Curie-Weiss law of equation (4) in the text with  $C = 1700$  K and  $T_0 = 71.3$  K. (b) The same data as in (a); the solid curve shows the quasi-one-dimensional chain model of equation (5) in the text, with parameters also given in the text. (c)  $x = 0.3$ ; the solid curve represents the Curie-Weiss law fitted to the experimental data between  $T_{c2} = 75.0$  K and  $T_x = 81.7$  K.

Polarization–electric field ( $P$ – $E$ ) hysteresis loops were measured by use of a programmable digital oscilloscope. A sine wave from the function generator (HP3310A) was amplified by a home-made power amplifier ( $\times 100$ ) and applied to the sample capacitor. The response signal of the crystal was fed to the digital oscilloscope (LeCroy 9420) through an operational amplifier (LF356) for data acquisition and processing, where the linear background was automatically subtracted as in the standard Sawyer–Tower circuit.

### 3. Experimental results and discussion

#### 3.1. The temperature dependence of the dielectric constant

In figure 1(a) we have shown the temperature dependence of the dielectric constant of  $\text{BP}_{0.6}\text{A}_{0.4}$  mixed crystal, where we can see a narrow region of Curie–Weiss behaviour before the antiferroelectric phase transition occurs at  $T_{c2} = 75.3$  K. The best-fitted curve shown in the figure obtained from the Curie–Weiss law

$$\epsilon_s = \frac{C}{T - T_0} \quad (4)$$

gives  $C = 1700$  K and  $T_0 = 71.3$  K. The experimental data show a distinct deviation from the best-fit curve in the temperature region above  $T_x = 82.5$  K. The region above  $T_x$  was best fitted by the quasi-1D Ising chain model previously applied to caesium dihydrogen phosphate [23, 24], BP [25], and BA [17]:

$$\epsilon_s = \epsilon_\infty + \frac{A}{T \exp(-2K_{\parallel}/T) - K_{\perp}}. \quad (5)$$

Here  $K_{\parallel}$  and  $K_{\perp}$  represent the intra- and inter-chain coupling constant, respectively. From the fitting of figure 1(b) we obtain  $A = 3.8 \times 10^6$  K,  $\epsilon_\infty = 44.7$ ,  $K_{\parallel} = 289.7$  K and  $K_{\perp} = -0.32$  K, which implies a strong ferroelectric coupling within the chain but a very weak antiferroelectric coupling between chains. In figure 1(c) the dielectric constant of  $\text{BP}_{0.7}\text{A}_{0.3}$  mixed crystal is shown as a function of temperature across the antiferroelectric phase transition at  $T_{c2} = 75.0$  K. The Curie–Weiss law again fits the experimental well data between  $T_{c2}$  and  $T_x (=81.7$  K), with  $C = 1174$  K and  $T_0 = 66.2$  K. Here again the sharp kink in the dielectric constant curve is clearly observed at  $T_x$ , which designates the 1D-to-3D dimensionality crossover.

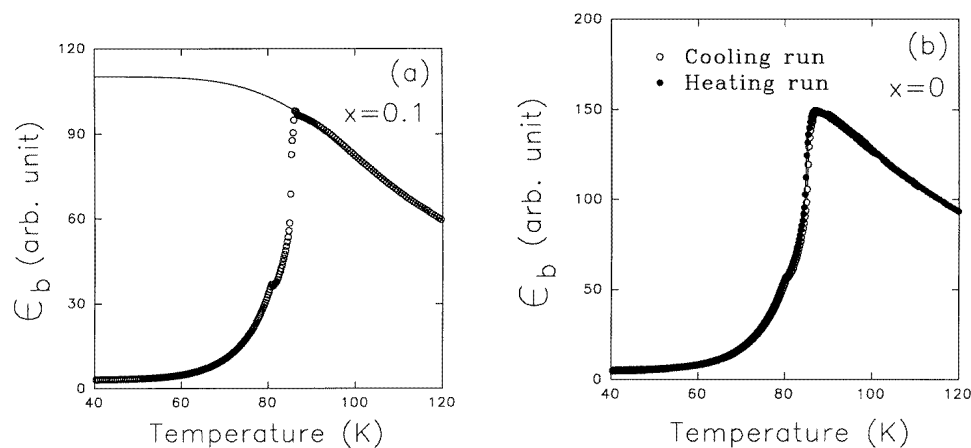


**Figure 2.** The temperature dependence of the quasi-static dielectric constant  $\epsilon_s$  for (a)  $\text{BP}_{0.9}\text{A}_{0.1}$  mixed crystal, and (b) pure BP. The solid curve in (a) shows the quasi-one-dimensional chain model of equation (5) in the text, fitted to the data above  $T_{c2} = 85.4$  K.

For  $\text{BP}_{0.9}\text{A}_{0.1}$  (figure 2(a)) and pure BP (figure 2(b)), however, the temperature dependence of the dielectric constants can be best fitted by the quasi-1D chain model all the way through to  $T_{c2}$ , although we can observe a cusp deviation starting at just  $T_{c2}$

for  $\text{BP}_{0.9}\text{A}_{0.1}$ . Clearly the 1D nature of BP is persistent to the point of antiferroelectric transition at the lower arsenate concentrations of  $x \leq 0.1$ .

In each of the sets of experimental data shown in figures 1 and 2, we could recognize another kink anomaly at a temperature ( $T_{c3}$ ) lower than that of the main phase transition at  $T_{c2}$ . These correspond to the unit-cell-doubling transition along the  $a$ -axis. For  $\text{BP}_{0.9}\text{A}_{0.1}$  and pure BP,  $T_{c3}$  was found at 81 K, below  $T_{c2}$  by less than 5 K. For  $\text{BP}_{0.6}\text{A}_{0.4}$  and  $\text{BP}_{0.7}\text{A}_{0.3}$ , on the other hand, the  $T_{c3}$ -anomaly was observed to be further away from  $T_{c2}$  and the corresponding cusps were more distinctive.

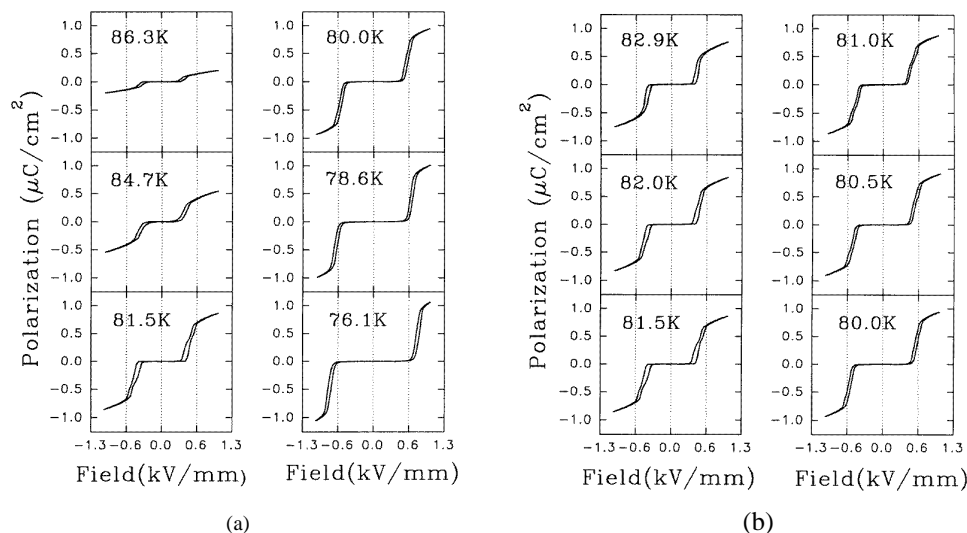


**Figure 3.** Polarization–electric field ( $P$ – $E$ ) double hysteresis loops observed for  $\text{BP}_{0.9}\text{A}_{0.1}$ , at temperatures (a) between 86.3 K and 76.1 K, and (b) between 82.9 K and 80.0 K (the  $T_{c3}$ -transition region) at a higher resolution of temperature.

At present we do not understand the nature of the interchain coupling and thus the microscopic origin of the dimensionality crossover. However, we can point out some hints based on the crystallographic data for BP and BA. From the structural data for BA [20] one can recognize that the two hydrogen atoms connecting carboxylic oxygens of betaine and arsenate oxygens are bound to the arsenate side, thus locating minus-one charge at the carboxylate group. Zwitterionicity of betaine is accomplished between this carboxylate group and the cationic centre at quaternary nitrogen. Certainly this very large dipole moment of betaine will act to enhance the interchain coupling efficiently. For BP, on the other hand, Schildkamp and Spilker found [3] that one of the hydrogen (deuterium) atoms connecting betaine and phosphate is disordered in the antiferrodistortive paraelectric phase, suggesting dynamical disorder of the proton (or deuterium) in this hydrogen bond. Larger acidity of phosphate explains the more delocalized nature of the proton. The zwitterionicity of betaine thus decreases. Reduced electrostatic interaction and also dynamical disorder will weaken the interchain coupling. This mechanism will contribute to maintaining the one-dimensionality of BP. When the concentration of BA increases above a threshold value in mixed crystals, the locally enhanced arsenate-to-arsenate interchain coupling caused by highly zwitterionic betaines will mediate the interaction between the whole chains. The dimensionality crossover phenomenon may thus take place when the lattice sum of the local interchain coupling exceeds a critical value for the collective long-range dipolar ordering.

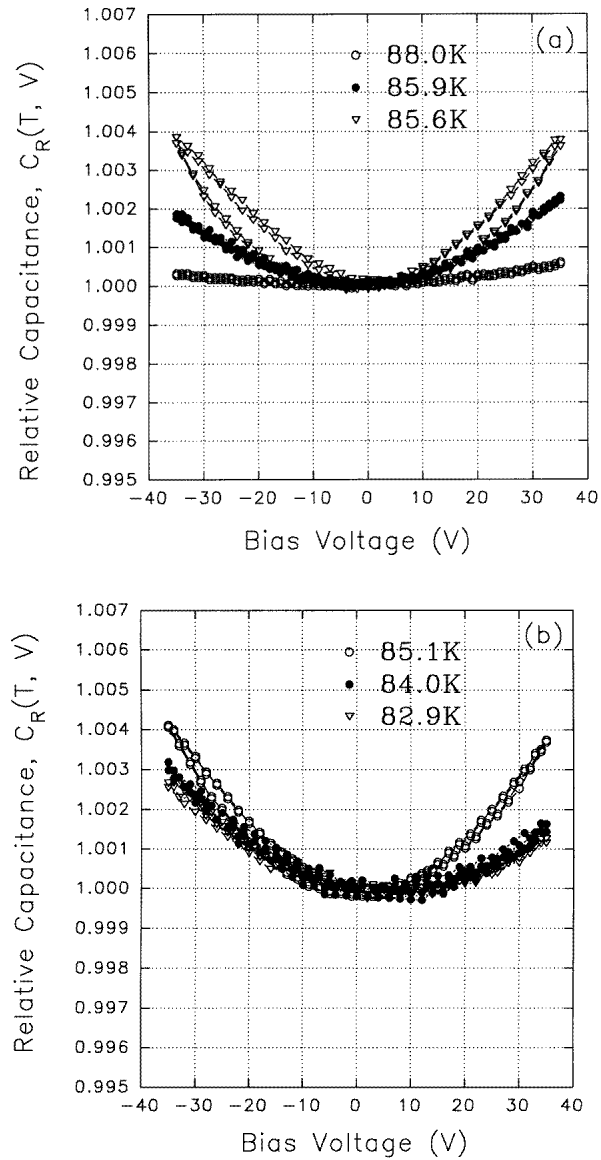


**Figure 4.** The relative capacitance,  $C_r(T, V_b) = C(T, V_b)/C(T, 0)$ , measured for  $\text{BP}_{0.9}\text{A}_{0.1}$ , as a function of temperature and d.c. bias voltage. (a)  $T > T_{c2}$ , (b)  $T_{c3} < T < T_{c2}$ , (c)  $T < T_{c3}$ , and (d) still lower temperatures down to 64.1 K.

This is, of course, expected to occur more easily in the mixed crystals with higher arsenate concentrations, as is observed in our experiment.

### 3.2. $P$ - $E$ hysteresis characteristics

Double hysteresis loops were observed for  $\text{BP}_{0.9}\text{A}_{0.1}$  as shown in figure 3, which confirms the antiferroelectric phase, and gives an estimation of the coercive fields  $E_c$  and sublattice

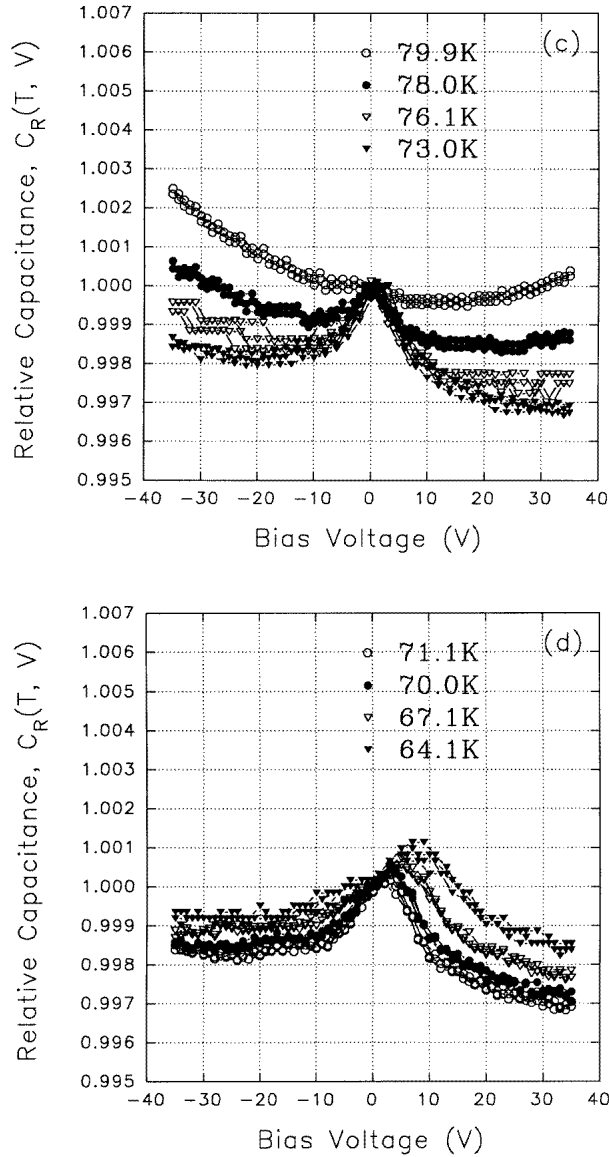


Figure 4. (Continued)

polarizations  $P_a$ . Near the lowest transition temperature  $T_{c3} = 81$  K we could observe in figure 3(a) a doubling distortion of the sublattice hysteresis loops, which was re-examined in more detail at higher temperature resolution as shown in figure 3(b). This is an observation of the electric-field-induced  $T_{c3}$ - (cell-doubling) phase transition from the high-temperature (before the cell doubling) antiferroelectric phase to the low-temperature (after the cell doubling) antiferroelectric phase. Though this phenomenon is observed only in a small range of temperature,  $82.0 \text{ K} < T < 80.5 \text{ K}$ , figure 3(b) shows clearly that the low-temperature phase ( $T < T_{c3}$ ) is more stabilized against the high-temperature phase ( $T > T_{c3}$ ) in the electric field, i.e.,  $\partial T_{c3} / \partial E > 0$  in the  $E$ - $T$  phase diagram. Electric field effects on the



dielectric anomaly at  $T_{c3}$  have already been studied by Hara *et al* [6], but they claimed no effect on the  $T_{c3}$ -transition temperature. The present hysteresis loop observation at a temperature very close to  $T_{c3}$  shows clearly that  $\partial T_{c3}/\partial E \neq 0$ , and has proved to be a more sensitive method of verifying such subtle effects.

### 3.3. The bias field effect on the dielectric constant

It has been reported for BP that above the critical field  $E_{cr} = 5.5 \text{ kV cm}^{-1}$  the field-induced ferroelectric transition takes place instead of the antiferroelectric transition [6, 13]. Hara *et al* [6] reported a bias field effect on the dielectric constant for field intensity above  $2.8 \text{ kV cm}^{-1}$ . As a first step in investigating the mechanism of this field-induced transition, we examined the effect of small bias field for  $\text{BP}_{0.9}\text{A}_{0.1}$ . We measured the ratio of  $C(T, V_b)$  to  $C(T, 0)$  as a function of the bias voltage, where  $C(T, V_b)$  denotes the capacitance of the  $\text{BP}_{0.9}\text{A}_{0.1}$  sample measured with a bias voltage  $V_b$  applied at temperature  $T$ . In figure 4 we have shown the relative capacitance,  $C_r(T, V_b) = C(T, V_b)/C(T, 0)$ , obtained at several temperatures between 88.0 K and 64.1 K. Figure 4(a) shows that we have no significant bias field effect above  $T_{c2}$  unless we come very close to  $T_{c2} = 85.4 \text{ K}$ . At temperatures between  $T_{c2}$  and  $T_{c3}$  (figure 4(b)) a quadratic increase of the relative capacitance with increasing bias field becomes apparent with a small asymmetry with respect to the direction of the bias field. Below  $T_{c3}$  (figure 4(c)) the asymmetry of the function  $C_r(T, V_b)$  with respect to  $V_b$  grows and gives double-well minima in  $C_r(T, V_b)$  with a local maximum appearing at zero bias field. On further decreasing the temperature below 73 K (figure 4(d)) the maximum in  $C_r(T, V_b)$  was observed to shift toward the  $V_b > 0$  side (e.g., 9 V at 64.1 K) and increasing bias field tends to make  $C_r(T, V_b) < 1$ . Since the bias field dependence of  $C_r$  reflects the nonlinear part of the dielectric constant, the temperature-dependent change in the nonlinear contribution, the quadratic term at temperatures  $T > T_{c3}$  and an additional quartic term at  $T < T_{c3}$  suggest a growing complexity of competing interactions. Though the microscopic origin for the competing interactions awaits further study, hydrogen bonding and the associated dynamics must be a key to understanding it because of the remarkable isotope effect on controlling the competition [10, 17]. Experimental work with microscopic probes such as magnetic resonance [26, 27] will contribute to solving the problem.

## 4. Conclusion

Betaine phosphate/arsenate ( $\text{BP}_{1-x}\text{A}_x$ ) mixed crystals are found to show the dimensionality crossover phenomena for  $x > 0.1$  before the antiferroelectric phase transition, and this phenomenon was interpreted by assuming that the arsenate groups tend to drive betaine groups toward the zwitterionic states and enhance the local interchain coupling.

A field-induced cell-doubling transition was observed in the hysteresis loop measurement, and an electric field dependence of  $T_{c3}$  was found—in contrast to the previous report. The electric bias field effect in  $\text{BP}_{1-x}\text{A}_x$  ( $x = 0.1$ ) was observed to show a qualitative change in the nonlinear dielectric response of the system as temperature was lowered from above  $T_{c2}$  to below  $T_{c3}$ , implying field-induced phase instability due to competing interactions.

More extensive studies using microscopic probes are required to explore the microscopic mechanism underlying the competing interactions being strongly dependent on temperature and electric bias field in the  $\text{BP}_{1-x}\text{A}_x$  systems.

## Acknowledgments

We thank Professors M Maeda, Y Ishibashi, and H Orihara for valuable discussion. This work was supported partly by the Japan–Korea Cooperative Research Programme, funded by the Ministry of Education, Science, Sports, and Culture, Japan. Support from the Korea Science and Engineering Foundation through the Centre for Molecular Science at KAIST is also appreciated.

## References

- [1] Albers J, Klöpperpieper A, Rother A J and Ehses K H 1982 *Phys. Status Solidi a* **74** 553
- [2] Albers J 1988 *Ferroelectrics* **78** 3
- [3] Schildkamp W and Spilker J 1984 *Z. Kristallogr.* **168** 159
- [4] Freitag O, Brückner H J and Unruh H-G 1985 *Z. Phys. B* **61** 75
- [5] Brückner H J, Unruh H-G, Fischer G and Genzel L 1988 *Z. Phys. B* **71** 225
- [6] Hara K, Umeda H, Ishibashi Y and Suzuki U 1989 *J. Phys. Soc. Japan* **58** 4215
- [7] Suzuki I, Ohta N and Maeda M 1989 *Ferroelectrics* **96** 225
- [8] Maeda M 1988 *J. Phys. Soc. Japan* **57** 3059
- [9] Maeda M, Atake T, Saito Y and Terauchi H 1989 *J. Phys. Soc. Japan* **58** 1135
- [10] Albers J, Klöpperpieper A, Müser H E and Rother H J 1984 *Ferroelectrics* **54** 45
- [11] Kroupa J and Albers J 1990 *Ferroelectrics* **108** 341
- [12] Launer S, Le Maire M, Schaack G and Haussuhl S 1992 *Ferroelectrics* **135** 217
- [13] Yasuda N and Konda J 1994 *Phys. Lett.* **185A** 495
- [14] Klöpperpieper K, Rother H J, Albers J and Ehses K H 1982 *Ferroelectr. Lett.* **44** 115
- [15] Maeda M 1988 *J. Phys. Soc. Japan* **57** 2162
- [16] Rother H J, Albers J, Klöpperpieper A and Müser H E 1985 *Japan. J. Appl. Phys. Suppl.* **2** **24** 384
- [17] Brückner H J 1989 *Z. Phys. B* **75** 259
- [18] Schell U 1985 *Ferroelectr. Lett.* **4** 123
- [19] Schell U and Müser H E 1987 *Z. Phys. B* **66** 237
- [20] Schildkamp W, Schäfer G and Spilker J 1984 *Z. Kristallogr.* **168** 187
- [21] Maeda M 1989 *Ferroelectrics* **96** 269
- [22] Maeda M and Suzuki I 1990 *Ferroelectrics* **108** 351
- [23] Blinc R, Zeks B, Levstik A, Filipic C, Slak J, Burger M, Zupacic I, Shuvalov L A and Baranov A 1979 *Phys. Rev. Lett.* **43** 231
- [24] Kojyo N and Onodera Y 1988 *J. Phys. Soc. Japan* **57** 4391
- [25] Fischer G, Brückner H J, Klöpperpieper A, Unruh H-G and Levstik A 1990 *Z. Phys. B* **79** 301
- [26] Ohki H, Nakamura N and Chihara H 1987 *Ferroelectr. Lett.* **8** 19
- [27] Nakamura N 1988 *Ferroelectrics* **78** 191